Title Page

Title:

Prognostic Significance of Mesothelin Expression in Colorectal Cancer Disclosed by Area-Specific Four-Point Tissue Microarrays

Authors' names:

Takehiro Shiraishi, MD[1], Eiji Shinto, MD, PhD[1], Ines P. Nearchou[2], BSc, Hitoshi Tsuda, MD, PhD[3], Yoshiki Kajiwara, MD, PhD[1], Takahiro Einama, MD, PhD[1], Peter D. Caie, PhD[2], Yoji Kishi, MD, PhD[1], Hideki Ueno, MD, PhD[1]

Authors' affiliations:

[1]Department of Surgery, National Defense Medical College, 3-2 Namiki, Tokorozawa, Saitama 359-0042, Japan

[2]Quantitative and Digital Pathology, School of Medicine, University of St. Andrews, St. Andrews, KY16 9TF, UK

[3]Department of Basic Pathology, National Defense Medical College, 3-2 Namiki, Tokorozawa, Saitama 359-0042, Japan

Corresponding author:

Eiji Shinto, M.D., Ph.D.

Department of Surgery, National Defense Medical College, 3-2 Namiki, Tokorozawa, Saitama 359-0042, Japan

Tel.: +81-42-995-1637; Fax: +81-42-996-5205; E-mail: shinto@ndmc.ac.jp

ORCID of the author:

Takehiro Shiraishi: 0000-0001-9150-2679

Total word count: 3366 words

Number of tables/figures: 2 tables and 4 figures

Supplementary figures: 0

Abstract

Mesothelin (MSLN) is a cell-surface glycoprotein present in many cancer types. Its expression is generally associated with an unfavorable prognosis. This study examined the prognostic significance of MSLN expression in different areas of individual colorectal cancers (CRCs) using tissue microarrays (TMAs) by enrolling 314 patients with stage II (T3-T4, N0, M0) CRCs. Using formalin-fixed paraffin-embedded tissue blocks from patients, TMA blocks were constructed. Tissue core specimens were obtained from submucosal invasive front [*Fr-sm*], subserosal invasive front [*Fr-ss*], central area [*Ce*], and rolled edge [*Ro*] of each tumor. Using these four-point TMA sets, MSLN expression was immunohistochemically surveyed. The area-specific prognostic significance of MSLN expression was evaluated. A deep-learning convolutional neural network algorithm was used for imaging analysis and evaluating our judgment's objectivity. MSLN staining ratio was positively correlated between the manual and machine-learning analyses (r = 0.71). The correlation coefficient between *Ro* and *Ce*, *Ro* and *Fr-sm*, and *Ro* and *Fr-ss* was r = 0.63, r = 0.54, and r = 0.61, respectively. Disease-specific survival curves for the MSLN-positive and MSLN-negative groups in *Fr-sm*, *Fr-ss*, and *Ro* were significantly different [five-year survival rates: 88.1% and 95.5% (P = 0.024), 85.0 and 96.2% (P = 0.0087), 87.8 and 95.5% (P = 0.051), and 77.9 and 95.8% (P = 0.046) for *Fr-sm*, *Fr-ss*, *Ce*, and *Ro*, respectively]. The analysis performed using area-specific four-point TMAs clearly demonstrated that MSLN expression in stage II CRC was relatively homogeneous within tumors. Additionally, high MSLN expression showed or tended to

show unfavorable prognostic significance regardless of the tumor area.

Keywords: mesothelin, colorectal cancer, tissue microarray, immunohistochemistry, artificial intelligence, deep learning

Abbreviation list

CI, Confidence interval; DSS, Disease-specific survival; HR, Hazard ratio; ROC, Receiver operating characteristic; TMA, Tissue microarray; EMT, Epithelial mesenchymal transition

Introduction

Colorectal cancer (CRC) cells emerge from the epithelial layer, and they proliferate and form a tumor mass, sequentially infiltrating into the submucosa, muscularis propria, and subserosa (Figure 1). The biological attitude of these cells gradually worsens with cancer invasion, and findings at the cancer's invasive front are strongly correlated with its malignancy potential [1-4]. However, superficial cancer cells are believed to retain their original characteristics at the beginning of tumor formation. Degeneration, apoptosis, and ulceration reduce this type of cancer cells. Of note, the characteristics of cancer development's early phase are likely to remain at the tumor's rolled edge. While this area is suitable for preoperative pathological examinations, its morphology is ineffectual at evaluating the biological attitude, due to a relatively monotonous histology, which may be diverted from the features at the invasive front closely reflecting cancer aggressiveness [5].

Mesothelin (MSLN) is a glycoprotein that is highly expressed in malignant tumors, such as malignant mesothelioma, pancreatic cancer, ovarian cancer, and lung adenocarcinoma [6, 7]. To date, the biological functions and molecular mechanisms of MSLN have not been clarified [8]. However, it has been shown in several reports that its expression is a promising parameter associated with poor prognosis or resistance to chemotherapy [9]. We previously examined immunohistochemical staining for the significance of MSLN expression in 530 cases of stage II/III CRC. Our study showed that its expression could be an independent prognostic factor [10]. During the evaluation of the immunostained sections, we observed a uniform immunoexpression of the MSLN-positive tumors

from the surface to the cancer's invasive front. Therefore, we concluded that overexpression of MSLN might represent an early phase change in cancer development. Such observation might be of high significance since MSLN could be preoperatively evaluated from biopsy specimens obtained from the tumor surface, therefore clarifying the patient's prognosis.

Tissue microarray (TMA) is a technique for high-throughput evaluation of protein expression. It uses a large number of archival tissue blocks collected for routine histopathological diagnosis [11]. We previously created a TMA by hollowing out the core from the submucosal invasive front, subserosal invasive front, central area, and the rolled edge of the tumor in primary T3 CRC tumors. Additionally, the area-specific significance of LN-5γ2 expression was evaluated by immunohistochemistry [12].

In recent years, applying machine learning on histopathological images has shown great potential for the objective and standardized analysis of prognostic features in various types of cancer [13-18]. We have previously shown that, using HALO® image analysis, we could quantitatively assess various prognostic features of the tumor microenvironment of stage II CRC [15].

In the present study, we investigated the clinical significance of MSLN expression in four different specific areas of 314 patients with stage II CRC who had undergone radical resection. We firstly assessed this by manual evaluation of the TMA slides. Subsequently, we applied a machine-learning approach using a HALO-AI™ deep-learning classifier to automatically analyze the images and evaluate the objectivity of our judgment.

Materials and Methods

Patient characteristics

First, the medical records of 314 patients with pathological stage II CRC were reexamined. Curatively resected and histologically proven stage II (T3-T4, N0, M0) CRCs were eligible [19]. Specifically, patients enrolled in the study underwent curative resection for CRC between January 1997 and December 2005 at our institution. These 314 patients were selected almost consecutively. The exclusion criteria were as follows: insufficient data regarding the outcome and histopathology or an insufficient volume of archival paraffin-embedded tissue blocks for TMA construction. None of the patients received preoperative chemotherapy or radiotherapy. Venous invasion and lymphatic invasion were recorded as negative or positive. Additionally, tumor budding was evaluated as per the Japanese Society for Cancer of the Colon and Rectum guidelines (2014) for the treatment of CRC [20]. During the follow-up, we observed that 22 (7.0%) patients died of CRC, with a median interval of 42.2 months (range: 6.0–88.4 months) from surgery to death. Additionally, 18 (5.7%) patients died of other diseases, with a median interval of 50.4 months (range: 4.9–121.6 months) after surgical treatment. The median follow-up period of the 274 survivors was 66.4 months (range: 35.7–133.3 months). With regard to adjuvant chemotherapies, 29 (9.2%) patients received adjuvant chemotherapy with 5-FU regimens. Table 1 shows the patient characteristics and CRCs' clinicopathological features. This study was performed following approval by the Ethics Committee

119 of the National Defense Medical College Hospital, Tokorozawa, Japan. Written informed consent for
120 the experimental use of tissue samples was provided by each patient based on institutional
121 regulations.

122

123 **TMA construction and immunohistochemical staining**

124 TMA was constructed as previously described [12, 21]. In brief, two regions of the
125 invasive front [submucosa (*Fr-sm*) and subserosa (*Fr-ss*)] and two regions of noninvasive frontal
126 lesions [central area (*Ce*) or superficial tumor area (rolled edge, *Ro*)] with viable cancer cells were
127 identified microscopically by referring to a whole section stained by hematoxylin and eosin (H&E).
128 In order to construct a TMA block, a single tissue core (diameter: 2.0 mm) was taken from each
129 region of formalin-fixed paraffin-embedded CRC tissue blocks ("donor" blocks) using a Tissue
130 Microarrayer (Beecher Instruments, Silver Spring, MD, USA). Cores were then transferred to the
131 "recipient" blocks (TMA blocks). Subsequently, the latter were cut to a 4 μm thickness. The obtained
132 sections were mounted on silane-coated glass slides, deparaffinized, and rehydrated in a graded
133 ethanol series. Antibody retrieval was heated for 15 min at 121°C in an autoclave at pH 9.0 using a
134 commercially available reagent kit (415211; Nichirei Bioscience, Tokyo, Japan). Sections were
135 incubated with a mouse monoclonal antibody against MSLN (clone 5B2 diluted 1 : 30; Novocastra,
136 Newcastle upon Tyne, UK) at a 1 : 30 dilution and reacted with a dextran polymer reagent combined
137 with secondary antibodies and peroxidase (EnVision+ System HRP; Dako, Glostrup, Denmark). The

anti-MSLN antibody used was raised against recombinant protein corresponding to the membrane-bound form of the MSLN molecule. One TMA block contained a maximum of 55 tissue cores and 24 TMA sets. A total of 1,256 core specimens were prepared for the present study. In our hospital, surgical resected specimens were fixed with 10% formalin neutral buffer solution for 1 to 4 days.

Manual pathological evaluation of MSLN expression

The TMA slides were independently evaluated by two observers (T. Shiraishi and E. Shinto). It is worth noting that the clinical outcomes were unknown to the observers. Of all cancer cells included in each tissue core, a percentage of immunopositive cancer cells were evaluated. The average of the two observers' scores was used as the final staining rate (Figure 2A, 2B, and 2C). In addition, a pathologist (H. Tsuda) evaluated the TMA slides and confirmed the reproducibility of the staining rate. Area-specific cutoffs were determined on the basis of receiver operating characteristic (ROC) curve analysis of death from CRC recurrence within five postoperative years. Upon the creation of the ROC curve, the area under the curve (AUC) of the portion below the curve of the graph was also calculated. The AUC had values ranging from 0 to 1. The closer the value was to 1, the higher the discriminability. With random discriminability, AUC = 0.5. The degree of interobserver agreement for the two observers was measured using a correlation analysis and generalized κ-test. In line with the criteria of Landis and Koch [22], κ-values were assigned a

157 strength-of-agreement score of poor (<0.00), slight (0.00–0.20), fair (0.21–0.40), moderate (0.41–
158 0.60), substantial (0.61–0.80), and near perfect (0.81–1.00). The correlation coefficient (r) for the
159 strength-of-agreement was assigned as follows: no correlation ($|r| < 0.3$), weak correlation ($0.3 \leq$
160 $|r| < 0.5$), moderate correlation ($0.5 \leq |r| < 0.7$), and strong correlation ($0.7 \leq |r|$).
161
162 **Pathological evaluation of MSLN expression using machine learning**
163 A total of 24 whole-slide TMA slides were captured with a 20× objective using a Leica
164 Aperio AT2 (Leica Microsystems, Wetzlar, Germany). For analysis, images in .svs file format were
165 uploaded into HALO® Next-Generation Image Analysis software (version 2.3.2089.34; Indica Labs,
166 Inc., Albuquerque, NM, USA). We utilized the software's TMA add-on for the segmentation of the
167 TMA cores. The HALO-AI™ deep-learning classifier add-on was used to train a classifier to segment
168 tumors from nontumor regions. Specifically, the classifier was trained on the basis of the manual
169 annotation of tumor and nontumor regions on 10 cores. The resolution was set to 0.75 μm/px, the
170 minimum object size was set to 20 μm^2 and the probability threshold was set to 70%. Then, the
171 trained deep-learning algorithm was applied across all TMA cores. Subsequently, the Cytonuclear
172 IHC (v.1.6) module was applied to classify MSLN-positive cells within the detected tumor regions.
173 Cell segmentation was performed based on the nuclear contrast threshold (0.515), minimum nuclear
174 OD (0.095), nuclear size (9.8, 571.7), nuclear segmentation aggressiveness (1) and minimum
175 cytoplasm radius (5). Cells were classified as MSLN-positive based on the cytoplasmic MSLN

positivity (stain minimum OD = 0.090, 0.287, 0.445; Figure 2D, 2E, and 2F).

Detection of mismatch repair deficiency

In the present study, we retrospectively verified the mismatch repair (MMR) protein status using immunohistochemical staining of MLH1 (Clone G168-15; BD Biosciences, San Jose, CA, USA) and MSH2 (FE11; Invitrogen, Carlsbad, CA, USA). Immunohistochemistry was performed as previously described [12]. Cancer cells were considered negative for protein expression only if they lacked staining in a sample in which healthy colonocytes and stroma cells were stained. The normal colonic crypt epithelium adjoining the tumor served as the internal control. When expressed, both MLH1 and MSH2 proteins positively stained the nuclei [23]. In particular, MMR protein status should be assessed via genetic testing based on the World Health Organization criteria. However, a previous study demonstrated that immunohistochemistry using MLH1 and MSH2 could accurately discriminate between MMR-deficient and MMR-proficient tumors. Marcus et al. reported that over 90% of MMR-deficient cases were predicted to have a mismatch repair gene defect using MLH1 and MSH2, and that all MSS cancers had intact staining with both antibodies [24]. Cancers negative for MLH1 or MSH2 were considered to have a DNA mismatch repair deficiency.

Statistical analysis

Correlations of MSLN expression scores and clinicopathological variables were calculated and tested for significance with χ^2 tests. Comparisons of continuous variables' differences with a normal distribution were performed using unpaired *t*-tests. Disease-specific survival (DSS) was defined as the interval between surgery and death from CRC recurrence. The word "recurrence" was used in this report to denote metachronous metastasis at the same site or in a different location. The Kaplan–Meier product limit method was used to calculate the survival probabilities. Additionally, comparisons were made using the log-rank test and the Akaike Information Criterion (AIC) was calculated [25]. Covariates with trend-significant effects ($P < 0.1$) on univariate analysis were selected for multivariate analysis of the survival factors. The significance of the association of clinical and pathological variables and postoperative survival was tested by Cox's proportional hazards regression. Specifically, this was used to determine both the hazard ratio (HR) and the 95% confidence interval. All statistical analyses were performed using JMP Pro 13.1.0 software (SAS Institute, Cary, NC, USA). We considered *P*-values of <0.05 as statistically significant.

Results

Correlations of immunohistochemical evaluation

Cancer cells' extent of MSLN immunostaining was independently evaluated both by two observers and by means of machine learning. An evaluation was performed for a total of 24 TMA

sets, comprising 1,256 core specimens. Strong positive correlations were found for the staining ratio of MSLN both between the two observers and between the manual and the machine-learning evaluation, with a correlation coefficient of r = 0.88 and r = 0.71, respectively (Figure 3A and 3B). Furthermore, it was confirmed that there was strong positive correlation between the average of the two observer's scores and that of the pathologist (H. Tsuda) (r = 0.78). The average value of the two observers was used to compare the staining ratio of MSLN in *Ro* and in three other different sites. The correlation coefficient between *Ro* and *Ce* was r = 0.63, between *Ro* and *Fr-sm* was r = 0.54, and between *Ro* and *Fr-ss* was r = 0.61, all of which were correlated (Figure 3C, 3D, and 3E).

Determination of the area-specific cutoff value for manual assessment results

The cutoff score was set at the respective site on the basis of a ROC curve analysis of death from CRC recurrence within five postoperative years. The cutoff values were 30% (AUC = 0.55) in *Fr-sm*, 25% (AUC = 0.58) in *Fr-ss*, 30% (AUC = 0.55) in *Ce*, and 45% (AUC = 0.59) in *Ro*.

Prognostic implications of MSLN status

< *Fr-sm* >

The interobserver agreement for the evaluation of MSLN immunostaining using a 30% cutoff was substantial (concordance rate: 94.4%, κ = 0.73). Cancers in the tissue cores were considered as MSLN-positive in 35 out of the 314 patients (11.1%) and MSLN-negative in 279

patients (88.9%). The 5-year DSS rates in patients with stage II CRC with MSLN-positive (88.1%) and MSLN-negative (95.5%) tumors were found to be significantly different (P = 0.024, AIC = 231) (Figure 4A). Table 2 shows the correlations of MSLN immunoreactivity and clinicopathological characteristics. Univariate analyses revealed a significant correlation between cancer death risk and depth of tumor (P = 0.011), tumor budding (P = 0.012), and MSLN positivity (P = 0.048). However, the Cox multivariate proportional hazards model analysis, which included variables with P < 0.1, showed an absence of an independent association between poor DSS and MSLN positivity (P = 0.22, HR = 0.53; Table 2).

< *Fr-ss* >

Using a 25% cutoff, the interobserver agreement for the evaluation of MSLN immunostaining was substantial (concordance rate: 90.8%, κ = 0.64). Among 314 patients, cancer in 41 (13.1%) was considered MSLN-positive and that in 273 patients (86.9%) was MSLN-negative. The 5-year DSS rates in patients with stage II CRC with MSLN-positive (85.0%) and MSLN-negative (96.2%) tumors were found to be significantly different (P = 0.0087, AIC = 229) (Figure 4B). There was a significant correlation between cancer death risk and MSLN positivity (P = 0.022) as seen by univariate analyses. Conversely, the Cox multivariate proportional hazards model analysis showed an absence of an independent association between poor DSS and MSLN positivity (P = 0.12, HR = 0.46; Table 2).

252

253 **< *Ce* >**

254 The interobserver agreement for the evaluation of MSLN immunostaining using a 30%
255 cutoff was near perfect (concordance rate: 97.4%, κ = 0.87). MSLN-positive cancer cases were 22
256 out of the 314 (7.0%) and MSLN-negative cases were 292 (93.0%). The 5-year DSS rates in patients
257 with stage II CRC with MSLN-positive (87.8%) and MSLN-negative (95.5%) tumors were different
258 (P = 0.051, AIC = 232) (Figure 4C). A marginally significant correlation was obtained between
259 cancer death risk and MSLN positivity (P = 0.087) in univariate analyses. However, an absence of
260 an independent association between poor DSS and MSLN positivity (P = 0.20, HR = 0.50; Table 2)
261 was observed in the Cox multivariate proportional hazards model analysis.

262

263 **< *Ro* >**

264 The interobserver agreement for the evaluation of MSLN immunostaining using a 45%
265 cutoff was substantial (concordance rate: 96.5%, κ = 0.74). Cancers were considered as
266 MSLN-positive and MSLN-negative in 33 (10.5%) and 281 patients (89.5%), respectively, out of
267 314 patients. In patients with stage II CRC with MSLN-positive (77.9%) and MSLN-negative
268 (95.8%) tumors, the 5-year DSS rates were significantly different (P = 0.046, AIC = 231) (Figure
269 4D). A marginally significant correlation between cancer death risk and MSLN positivity was
270 revealed in univariate analyses (P = 0.089), but the Cox multivariate proportional hazards model

analysis showed that MSLN positivity remained as the only variable independently associated with poor DSS (P = 0.049, HR = 0.28; Table 2).

Discussion

It has been suggested in recent reports that high MSLN expression in pancreatic, ovarian, and gastric cancers may be a poor prognostic factor [9, 26-29]. In these studies, examination of MSLN expression was performed for various carcinomas using whole tissue sections. Of note, in the present study, the degree of MSLN expression was evaluated by immunohistochemistry using TMA of stage II CRC. In particular, we focused on MSLN expression's clinical significance at different sites of the cancer tissue. As a result, our study demonstrates that cases with high MSLN expression at four sites (i.e., *Fr-sm*, *Fr-ss*, *Ce*, and *Ro*) had poor prognosis. Importantly, MSLN expression can reflect prognosis not only in the invasive front of the tumor (i.e., *Fr-sm* and *Fr-ss*), but also in the tumor surface area (i.e., *Ro*). Additionally, MSLN expression in each portion is highly correlated. These results suggest that the grade of cancer aggressiveness can be evaluated in preoperative endoscopic biopsy tissues. Indeed, T classification and tumor budding are strong prognostic factors; however, these indicators cannot be accurately assessed before surgical treatment. This finding is worth noting when considering its clinical application.

Currently, molecular targeted therapy is indicated for the treatment of diverse cancers. Recently approved therapies include antibodies against epidermal growth factor receptors (EGFRs), such as

290 cetuximab and panitumumab, and against vascular endothelial growth factors for CRC [30-32].
291 MSLN, a cell-membrane-binding protein similar to EGFR, may become a candidate target for
292 antibody therapy. Currently, MSLN is being tested as a target of antibody-mediated pancreatic
293 cancer therapy [33]. The overexpression ratio of MSLN in CRC is lower compared with pancreatic
294 cancer; however, it is possible that, in the future, MSLN expression in CRC will be indicated for
295 antibody therapy, considering the marked impact of MSLN expression. This study suggests that the
296 expression of MSLN in CRC can be evaluated in endoscopic biopsy tissues. This finding is a key
297 implication of our study, showing that it may be possible to obtain accurate information associated
298 with the treatment strategy prior to radical resection or even when a tumor is surgically unresectable.
299 Although, the present study was conducted on patients with stage II CRC, future studies are
300 necessary to examine the similarity in MSLN expression among biopsy specimens, primary lesions,
301 and metastatic sites in stage IV CRC. Among the 33 recurrent cases in our cohort, homogeneous
302 MSLN expression was also observed (r = 0.64 (*Ro* vs. *Ce*), r = 0.69 (*Ro* vs. *Fr-sm*), r = 0.69 (*Ro*
303 vs. *Fr-ss*)), which may support our treatment strategy.

304 Epithelial mesenchymal transition (EMT) is known to be strongly associated with tumor
305 infiltration [34]. Previous reports suggested that MSLN may be a constituent molecule of EMT and
306 is involved in tumor progression and metastasis [35]. Indeed, MSLN has a strong correlation with
307 tumor budding, a plausible morphological phenotype of EMT [36, 37]. However, MSLN expression
308 was correlated with budding grades both in the invasive front of a tumor and in the tumor surface

309 region (data not shown). Additionally, the MSLN expression ratios were almost the same in all four
310 areas. Thus, we consider that MSLN is not a molecule that appears along with EMT promotion,
311 while it may be associated with induction into EMT. If antibody therapy to MSLN becomes a
312 treatment choice, EMT could be blocked at the upstream of the cascade, potentially leading to broad
313 suppression of invasive activities.

314 We have previously reported that MSLN expression was selected as a strong independent
315 prognostic factor in stage II/III CRC using standard sections [10]. In the present study, high MSLN
316 expression could not be estimated to be an independent poor prognostic factor at three sites, namely,
317 *Fr-sm*, *Fr-ss*, and *Ce*. The exclusive advantage of TMA is that data from many cases can be
318 efficiently obtained. Of note, a recent report showed that no difference was obtained between TMA
319 cores and whole sections in immunoexpression grades of prognostic markers [38]. However, it is
320 necessary to recognize that a narrow observation range may represent a limitation, particularly when
321 examining CRC.

322 The application of deep-learning and automated image analysis in the field of pathology is
323 continuously increasing, and has previously been characterized as the third revolution in pathology
324 [39]. By evaluating H&E-stained whole-slide sections, HALO-AI™ has been shown to be able to
325 detect different types of cells and tissues [40, 41]. In the present study, we generated a single
326 algorithm via training on the basis of the manual annotation of tumor and nontumor regions on 10
327 cores that were immunohistochemically stained for MSLN. This was subsequently applied, with

328 constant thresholds, across the entire cohort to classify tumors from nontumor regions and to
329 evaluate the MSLN positivity of the tumor cells without any human subjectivity. The correlation
330 between manual and machine-learning evaluation of the MSLN staining ratio was found to be strong.
331 Such observations suggest that the fair objectivity of human judgment was verified and that this
332 machine-learning approach is promising for the evaluation of protein expression on
333 immunohistochemically stained slides.

334 There were some limitations in the present study. First, there were potential changes in tissue
335 MSLN antigenicity associated with tissue processing (e.g., fixation, section preparation, especially
336 through TMA block construction). These changes could have resulted in insufficient detection
337 sensitivity. Second, factors such as the retrospective study design, postoperative adjuvant
338 chemotherapy, surgical procedures, and/or treatments for recurrent cases that were influenced by the
339 age or performance status may have acted as sources of bias.

340 In conclusion, in the present study, TMA analyses demonstrated that the expression of MSLN in
341 stage II CRC was relatively homogeneous within a tumor, and high MSLN expression showed or
342 tended to show unfavorable prognostic significance regardless of the tumor area. Such findings
343 suggest that this molecule could be fit for the evaluation of endoscopic biopsy tissues.
344 Chemotherapy has opened new avenues for drastically downsizing and downstaging advanced
345 cancers. However, how to predict these effects is currently under study. Our novel findings may
346 contribute to advances toward a truly customized selection of preoperative antibody treatments based

347 on MSLN expression.

348

Compliance with ethical standards

The experiments reported here were performed in agreement with the Declaration of Helsinki principles and with the Ethics Committee of the National Defense Medical College Hospital, Tokorozawa, Japan. ES is the guarantor of this work and, as such, had full access to all of the data in the study and takes responsibility for the integrity of the data and the accuracy of the data analysis.

Conflict of interest statement

The authors have no conflicts of interest to declare.

Funding

I.P.N. is the recipient of a Medical Research Scotland PhD Studentship awarded to P.D.C. Indica Labs, Inc. provided in-kind resource.

Authors' contributions

TS and ES conceived and designed the experiments. TS and IPN performed the experiments. IPN performed the digital image analysis. TS, ES, and HT analyzed the histopathological data. TS, ES, and IPN drafted the manuscript. YK, TE, PDC, YK, and HU revised the manuscript. TS finalized the manuscript. All authors reviewed and approved the manuscript.

368 **References**

369 1. Jass JR, Love SB, Northover JM (1987) A New Prognostic Classification of Rectal Cancer. Lancet
370 1:1303-1306. https://doi.org/10.1016/s0140-6736(87)90552-6

371 2. Ono M, Sakamoto M, Ino Y, Moriya Y, Sugihara K, Muto T, Hirohashi S (1996) Cancer Cell
372 Morphology at the Invasive Front and Expression of Cell Adhesion-Related Carbohydrate in the
373 Primary Lesion of Patients with Colorectal Carcinoma with Liver Metastasis. Cancer 78:1179-1186.
374 https://doi.org/10.1002/(SICI)1097-0142(19960915)78:6<1179::AID-CNCR3>3.0.CO;2-5

375 3. Hase K, Shatney C, Johnson D, Trollope M, Vierra M (1993) Prognostic Value of Tumor "Budding"
376 in Patients with Colorectal Cancer. Dis Colon Rectum 36:627-635.
377 https://doi.org/10.1007/bf02238588

378 4. Ueno H, Murphy J, Jass JR, Mochizuki H, Talbot IC (2002) Tumour 'Budding' as an Index to
379 Estimate the Potential of Aggressiveness in Rectal Cancer. Histopathology 40:127-132.
380 https://doi.org/10.1046/j.1365-2559.2002.01324.x

381 5. Talbot IC, Ritchie S, Leighton M, Hughes AO, Bussey HJ, Morson BC (1981) Invasion of Veins by
382 Carcinoma of Rectum: Method of Detection, Histological Features and Significance. Histopathology
383 5:141-163. https://doi.org/10.1111/j.1365-2559.1981.tb01774.x

384 6. Ordonez NG (2003) Value of mesothelin immunostaining in the diagnosis of mesothelioma, Mod
385 Pathol 16:192-197. https://doi.org/10.1097/01.MP.0000056981.16578.C3

386 7. Frierson HF, Jr., Moskaluk CA, Powell SM, Zhang H, Cerilli LA, Stoler MH, Cathro H, Hampton

GM (2003) Large-scale molecular and tissue microarray analysis of mesothelin expression in common human carcinomas, Hum Pathol 34:605-609. https://doi.org/10.1016/S0046-8177(03)00177-1

8. Bera TK, Pastan I (2000) Mesothelin is not Required for Normal Mouse Development or Reproduction. Mol Cell Biol 20:2902-2906. https://doi.org/10.1128/mcb.20.8.2902-2906.2000

9. Cheng WF, Huang CY, Chang MC, Hu YH, Chiang YC, Chen YL, Hsieh CY, Chen CA (2009) High Mesothelin Correlates with Chemoresistance and Poor Survival in Epithelial Ovarian Carcinoma. Br J Cancer 100:1144-1153. https://doi.org/10.1038/sj.bjc.6604964

10. Shiraishi T, Shinto E, Mochizuki S, Tsuda H, Kajiwara Y, Okamoto K, Einama T, Hase K, Ueno H (2019) Mesothelin Expression has Prognostic Value in Stage II/III Colorectal Cancer. Virchows Arch 474:297-307. https://doi.org/10.1007/s00428-018-02514-4

11. Kononen J, Bubendorf L, Kallioniemi A, Barlund M, Schraml P, Leighton S, Torhorst J, Mihatsch MJ, Sauter G, Kallioniemi OP (1998) Tissue Microarrays for High-throughput Molecular Profiling of Tumor Specimens. Nat Med 4:844-847. https://doi.org/10.1038/nm0798-844

12. Shinto E, Tsuda H, Ueno H, Hashiguchi Y, Hase K, Tamai S, Mochizuki H, Inazawa J, Matsubara O (2005) Prognostic Implication of Laminin-5 Gamma 2 Chain Expression in the Invasive Front of Colorectal Cancers, Disclosed by Area-specific Four-point Tissue Microarrays. Lab Invest 85:257-266. https://doi.org/10.1038/labinvest.3700199

13. Caie PD, Turnbull AK, Farrington SM, Oniscu A, Harrison DJ (2014) Quantification of Tumour Budding, Lymphatic Vessel Density and Invasion Through Image Analysis in Colorectal Cancer. J Transl Med 12:156. https://doi.org/10.1186/1479-5876-12-156

14. Caie PD, Zhou Y, Turnbull AK, Oniscu A, Harrison DJ (2016) Novel Histopathologic Feature Identified through Image Analysis Augments Stage II Colorectal Cancer Clinical Reporting. Oncotarget 7:44381-44394. https://doi.org/10.18632/oncotarget.10053

15. Nearchou IP, Lillard K, Gavriel CG, Ueno H, Harrison DJ, Caie PD (2019) Automated Analysis of Lymphocytic Infiltration, Tumor Budding, and Their Spatial Relationship Improves Prognostic Accuracy in Colorectal Cancer. Cancer immunology research 7:609-620. https://doi.org/10.1158/2326-6066.CIR-18-0377

16. Balkenhol MCA, Bult P, Tellez D, Vreuls W, Clahsen PC, Ciompi F, van der Laak J (2019) Deep Learning and Manual Assessment Show that the Absolute Mitotic Count does not Contain Prognostic Information in Triple Negative Breast Cancer. Cell Oncol 42:555-569. https://doi.org/10.1007/s13402-019-00445-z

17. Brieu N, Gavriel CG, Nearchou IP, Harrison DJ, Schmidt G, Caie PD (2019) Automated Tumour Budding Quantification by Machine Learning Augments TNM Staging in Muscle-Invasive Bladder Cancer Prognosis. Sci Rep 9:5174. https://doi.org/10.1038/s41598-019-41595-2

18. Lucas M, Jansen I, Savci-Heijink CD, Meijer SL, de Boer OJ, van Leeuwen TG, de Bruin DM, Marquering HA (2019) Deep Learning for Automatic Gleason Pattern Classification for Grade

Group Determination of Prostate Biopsies. Virchows Arch 475:77-83. https://doi.org/10.1007/s00428-019-02577-x

19. Brierley J, Gospodarowicz MK, Wittekind C. TNM Classification of Malignant Tumours. New York, Wiley-Liss, 2017, pp. 73-76

20. Watanabe T, Itabashi M, Shimada Y, Tanaka S, Ito Y, Ajioka Y, Hamaguchi T, Hyodo I, Igarashi M, Ishida H, Ishihara S, Ishiguro M, Kanemitsu Y, Kokudo N, Muro K, Ochiai A, Oguchi M, Ohkura Y, Saito Y, Sakai Y, Ueno H, Yoshino T, Boku N, Fujimori T, Koinuma N, Morita T, Nishimura G, Sakata Y, Takahashi K, Tsuruta O, Yamaguchi T, Yoshida M, Yamaguchi N, Kotake K, Sugihara K, Japanese Society for Cancer of the C, Rectum: Japanese Society for Cancer of the Colon and Rectum (JSCCR) (2015) Guidelines 2014 for Treatment of Colorectal Cancer. Int J Clin Oncol 20:207-239. https://doi.org/10.1007/s10147-015-0801-z

21. Yamadera M, Shinto E, Tsuda H, Kajiwara Y, Naito Y, Hase K, Yamamoto J, Ueno H (2018) Sialyl Lewis(x) Expression at the Invasive Front as a Predictive Marker of Liver Recurrence in Stage II Colorectal Cancer. Oncol Lett 15:221-228. https://doi.org/10.3892/ol.2017.7340

22. Landis JR, Koch GG: The Measurement of Observer Agreement for Categorical Data. Biometrics 1977, 33:159-174.

23. Christensen M, Katballe N, Wikman F, Primdahl H, Sorensen FB, Laurberg S, Orntoft TF (2002) Antibody-based Screening for Hereditary Nonpolyposis Colorectal Carcinoma Compared with Microsatellite Analysis and Sequencing. Cancer 95:2422-2430. https://doi.org/10.1002/cncr.10979

24. Marcus VA, Madlensky L, Gryfe R, Kim H, So K, Millar A, Temple LK, Hsieh E, Hiruki T, Narod S, Bapat BV, Gallinger S, Redston M (1999) Immunohistochemistory for hMLH1 and hMSH2: a practical test for DNA mismatch repair-deficient tumors. Am J Surg Pathol 23:1248-1255. https://doi.org/10.1097/00000478-199910000-00010

25. Akaike H (1974) A New Look at the Statistical Model Identification. IEEE Trans Automat Control 19:716-722.

26. Baba K, Ishigami S, Arigami T, Uenosono Y, Okumura H, Matsumoto M, Kurahara H, Uchikado Y, Kita Y, Kijima Y, Kitazono M, Shinchi H, Ueno S, Natsugoe S (2012) Mesothelin Expression Correlates with Prolonged Patient Survival in Gastric Cancer. J Surg Oncol 105:195-199. https://doi.org/10.1002/jso.22024

27. Einama T, Homma S, Kamachi H, Kawamata F, Takahashi K, Takahashi N, Taniguchi M, Kamiyama T, Furukawa H, Matsuno Y, Tanaka S, Nishihara H, Taketomi A, Todo S (2012) Luminal Membrane Expression of Mesothelin is a Prominent Poor Prognostic Factor for Gastric Cancer. Br J Cancer 107:137-142. https://doi.org/10.1038/bjc.2012.235

28. Li M, Bharadwaj U, Zhang R, Zhang S, Mu H, Fisher WE, Brunicardi FC, Chen C, Yao Q (2008) Mesothelin is a Malignant Factor and Therapeutic Vaccine Target for Pancreatic Cancer. Mol Cancer Ther 7:286-296. https://doi.org/10.1158/1535-7163.MCT-07-0483

460 29. Yen MJ, Hsu CY, Mao TL, Wu TC, Roden R, Wang TL, Shih Ie M (2006) Diffuse Mesothelin
461 Expression Correlates with Prolonged Patient Survival in Ovarian Serous Carcinoma. Clin Cancer
462 Res 12:827-831. https://doi.org/10.1158/1078-0432.CCR-05-1397
463 30. Bokemeyer C, Bondarenko I, Makhson A, Hartmann JT, Aparicio J, de Braud F, Donea S, Ludwig
464 H, Schuch G, Stroh C, Loos AH, Zubel A, Koralewski P (2009) Fluorouracil, Leucovorin, and
465 Oxaliplatin with and without Cetuximab in the First-line Treatment of Metastatic Colorectal Cancer.
466 J Clin Oncol 27:663-671. https://doi.org/10.1200/JCO.2008.20.8397
467 31. Van Cutsem E, Kohne CH, Hitre E, Zaluski J, Chang Chien CR, Makhson A, D'Haens G, Pinter T,
468 Lim R, Bodoky G, Roh JK, Folprecht G, Ruff P, Stroh C, Tejpar S, Schlichting M, Nippgen J,
469 Rougier P (2009) Cetuximab and Chemotherapy as Initial Treatment for Metastatic Colorectal
470 Cancer. N Engl J Med 360:1408-1417. https://doi.org/10.1056/NEJMoa0805019
471 32. Saltz LB, Clarke S, Diaz-Rubio E, Scheithauer W, Figer A, Wong R, Koski S, Lichinitser M, Yang
472 TS, Rivera F, Couture F, Sirzen F, Cassidy J (2008) Bevacizumab in Combination with
473 Oxaliplatin-based Chemotherapy as First-line Therapy in Metastatic Colorectal Cancer: A
474 Randomized Phase III Study. J Clin Oncol 26:2013-2019. https://doi.org/10.1200/JCO.2007.14.9930
475 33. Hassan R, Thomas A, Alewine C, Le DT, Jaffee EM, Pastan I (2016) Mesothelin Immunotherapy
476 for Cancer: Ready for Prime Time? J Clin Oncol 34:4171-4179.
477 https://doi.org/10.1200/JCO.2016.68.3672

34. Hanahan D, Weinberg RA: Hallmarks of Cancer (2011) The Next Generation. Cell 144:646-674. https://doi.org/10.1016/j.cell.2011.02.013

35. He X, Wang L, Riedel H, Wang K, Yang Y, Dinu CZ, Rojanasakul Y (2017) Mesothelin Promotes Epithelial-to-mesenchymal Transition and Tumorigenicity of Human Lung Cancer and Mesothelioma Cells. Mol Cancer 16:63. https://doi.org/10.1186/s12943-017-0633-8

36. Brabletz T, Jung A, Spaderna S, Hlubek F, Kirchner T (2005) Opinion: Migrating Cancer Stem Cells - An Integrated Concept of Malignant Tumour Progression. Nat Rev Cancer 5:744-749. https://doi.org/10.1038/nrc1694

37. Karagiannis GS, Poutahidis T, Erdman SE, Kirsch R, Riddell RH, Diamandis EP (2012) Cancer-associated Fibroblasts Drive the Progression of Metastasis through Both Paracrine and Mechanical Pressure on Cancer Tissue. Mol Cancer Res 10:1403-1418. https://doi.org/10.1158/1541-7786.MCR-12-0307

38. Ono M, Tsuda H, Yunokawa M, Yonemori K, Shimizu C, Tamura K, Kinoshita T, Fujiwara Y (2015) Prognostic Impact of Ki-67 Labeling Indices with 3 Different Cutoff Values, Histological Grade, and Nuclear Grade in Hormone-receptor-positive, HER2-negative, Node-negative Invasive Breast Cancers. Breast Cancer 22:141-152. https://doi.org/10.1007/s12282-013-0464-4

39. Salto-Tellez M, Maxwell P, Hamilton P (2019) Artificial Intelligence-The Third Revolution in Pathology. Histopathology 74:372-376. https://doi.org/10.1111/his.13760

40. Martin DR, Hanson JA, Gullapalli RR, Schultz FA, Sethi A, Clark DP (2019) A Deep Learning Convolutional Neural Network can Recognize Common Patterns of Injury in Gastric Pathology. Arch Pathol Lab Med 2019. https://doi.org/10.5858/arpa.2019-0004-OA

41. Bui MM, Asa SL, Pantanowitz L, Parwani A, van der Laak J, Ung C, Balis U, Isaacs M, Glassy E, Manning L (2019) Digital and Computational Pathology: Bring the Future into Focus. J Pathol Inform 10:10.

503 **Figure Legends**

504

505 **Figure 1:** Illustration of time-course changes of CRC formation and sampling sites used for TMA
506 construction in the present study.

507

508 The four areas comprise the submucosal invasive front (*Fr-sm*), subserosal invasive front (*Fr-ss*),
509 central area (*Ce*), and rolled edge (*Ro*).

510

511 **Figure 2:** Characteristic microscopic appearance of MSLN expression and machine learning
512 workflow for the evaluation of MSLN in CRC tissues.

513

514 (A) MSLN-negative tissue with no stained cells. (B) Positive staining localized at the apical regions
515 of the cells at the endoluminal surface. (C) Positive staining in cytoplasmic deposits or granules. (D)
516 Raw image, (E) Tumor-to-stroma segmentation, (F) MSLN-positive cell quantification within the
517 tumor areas (tumor cells are shown in blue; tumor cells positive for MSLN are shown in yellow).
518 (Magnification: A, B, C, 200×; D, E, F, 20×). MSLN; mesothelin.

519

520 **Figure 3:** Correlations of immunohistochemical evaluation.

521

(A) A very strong positive correlation was found for the staining ratio of MSLN between the two observers, with a correlation coefficient of r = 0.88. (B) A very strong positive correlation was found for the staining ratio of MSLN between the manual and the machine-learning, with a correlation coefficient of r = 0.71. (C, D, E) The correlation coefficient of the staining ratio of MSLN evaluated by the manual between *Ro* and *Ce* was r = 0.63, between *Ro* and *Fr-sm* was r = 0.54, and between *Ro* and *Fr-ss* was r = 0.61, showing a correlation. MSLN: mesothelin.

Figure 4: MSLN status's Kaplan–Meier survival estimates according to cancer areas.

(A) MSLN-negative versus MSLN-positive tissue in the submucosal invasive front (*Fr-sm*). The difference in the 5-year DSS (88.1 versus 95.5%) was significant (P = 0.024, AIC = 231). (B) MSLN-negative versus MSLN-positive tissue in the subserosal invasive front (*Fr-ss*). The difference in the 5-year DSS (85.0 versus 96.2%) was significant (P = 0.0087, AIC = 229). (C) MSLN-negative versus MSLN-positive tissue in the central area (*Ce*). The difference in the 5-year DSS (87.8 versus 95.5%) tends to be significant (P = 0.051, AIC = 232). (D) MSLN-negative versus MSLN-positive tissue in the rolled edge (*Ro*). The difference in the 5-year DSS (77.9 versus 95.8%) was significant (P = 0.046, AIC = 231). MSLN: mesothelin.

Figure 1

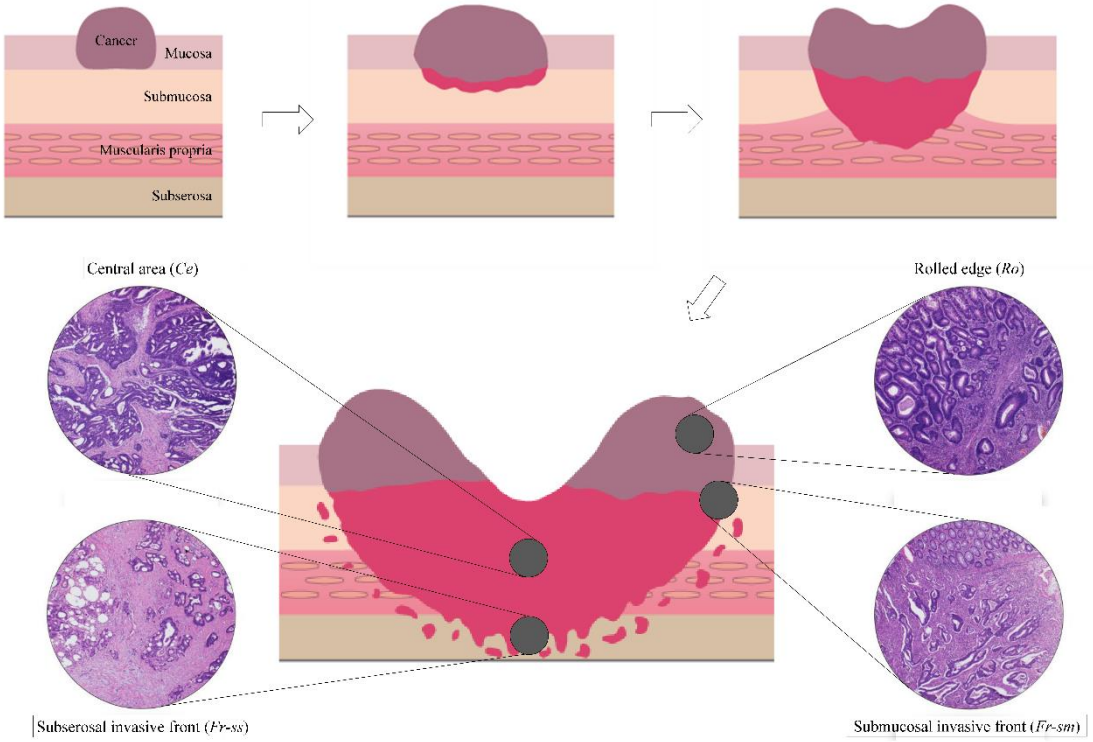
Cancer
Mucosa
Submucosa
Muscularis propria
Subserosa
Central area (Ce)
Rolled edge (Ro)
Subserosal invasive front (Fr-ss)
Submucosal invasive front (Fr-sm)

Figure 2

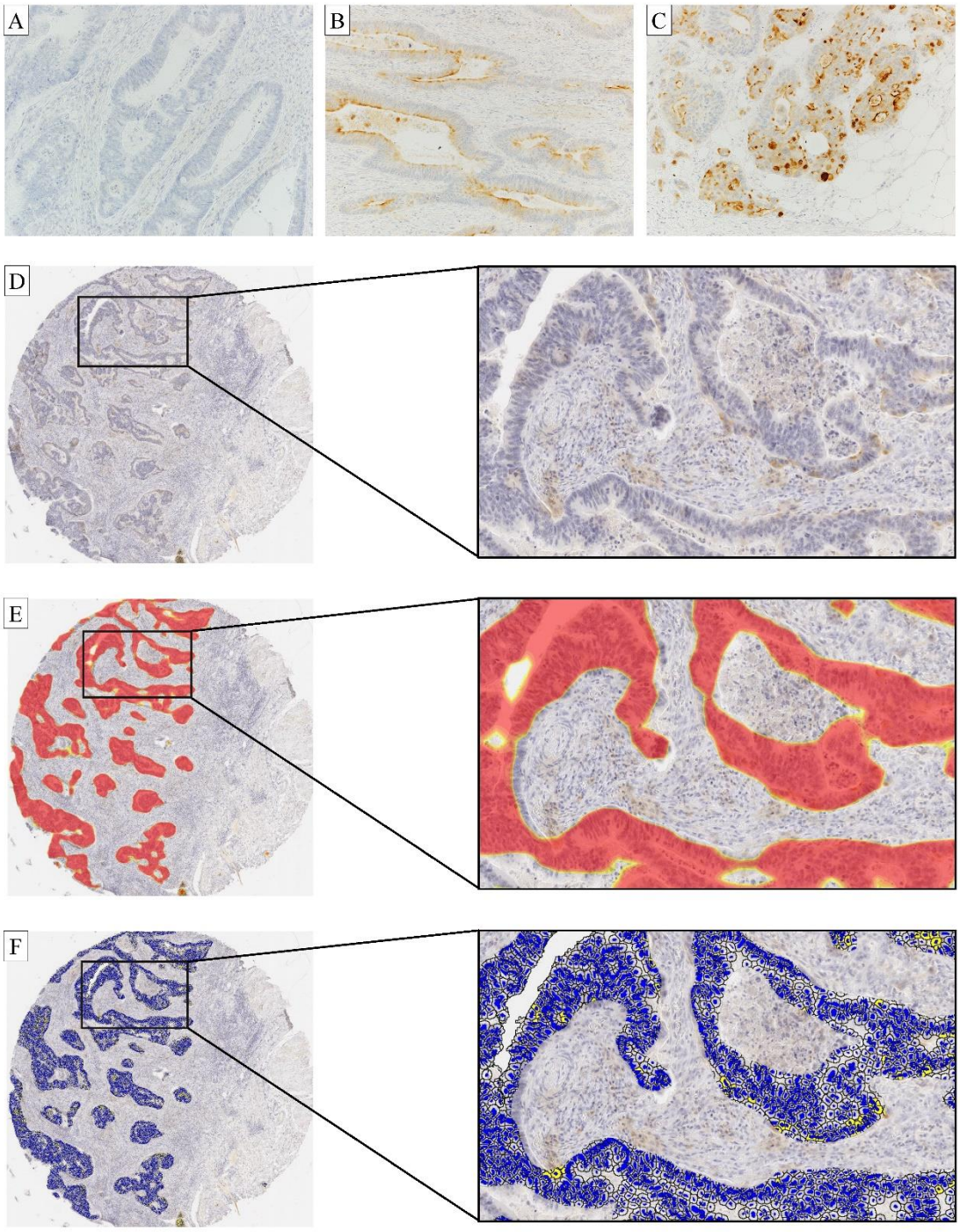

553

554

555

Figure 3

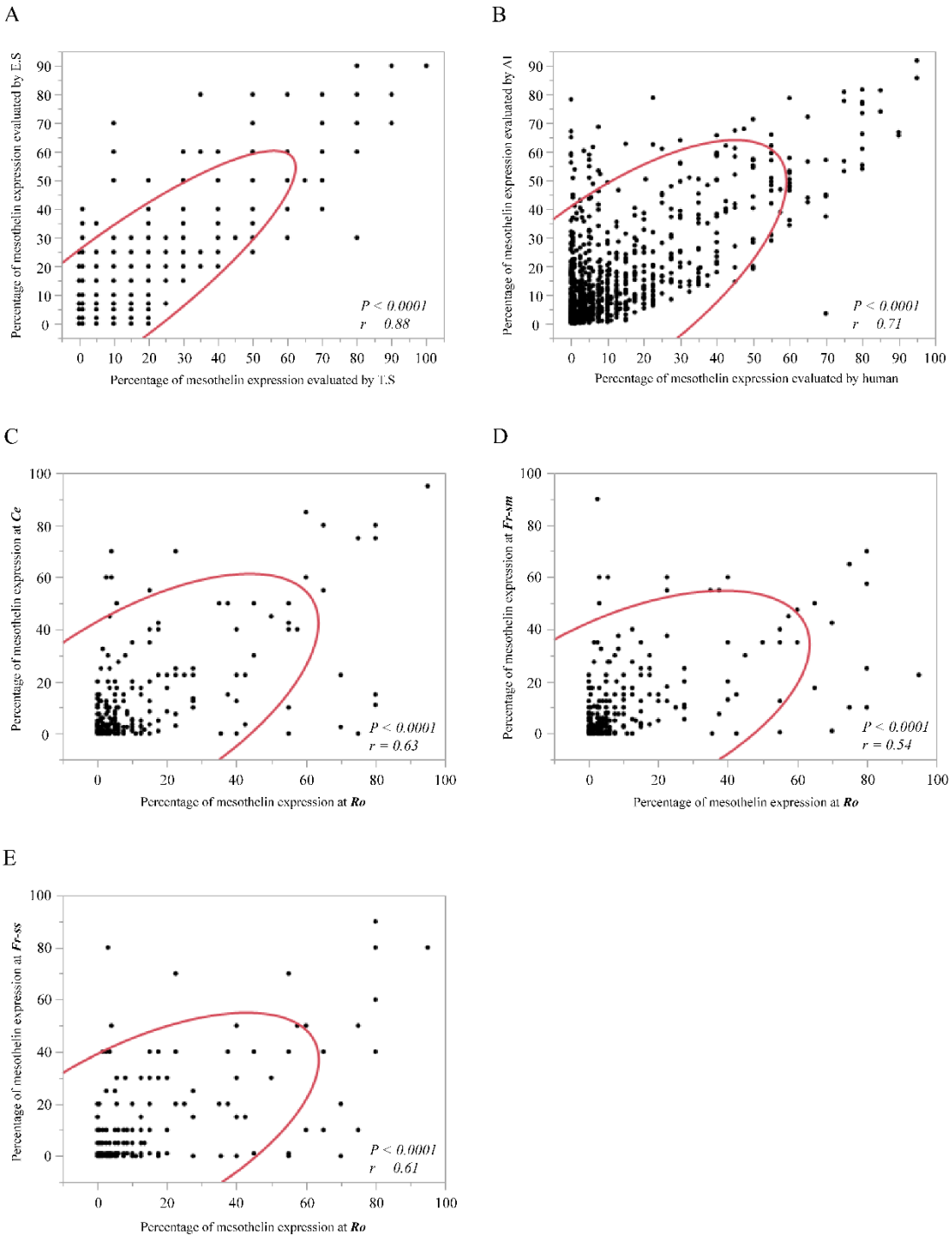
A
Percentage of mesothelin expression evaluated by E.S
Percentage of mesothelin expression evaluated by T.S
P < 0.0001
r 0.88
B
Percentage of mesothelin expression evaluated by AI
Percentage of mesothelin expression evaluated by human
P < 0.0001
r 0.71
C
Percentage of mesothelin expression at Ce
Percentage of mesothelin expression at Ro
P < 0.0001
r = 0.63
D
Percentage of mesothelin expression at Fr-sm
Percentage of mesothelin expression at Ro
P < 0.0001
r = 0.54
E
Percentage of mesothelin expression at Fr-ss
Percentage of mesothelin expression at Ro
P < 0.0001
r 0.61

Figure 4

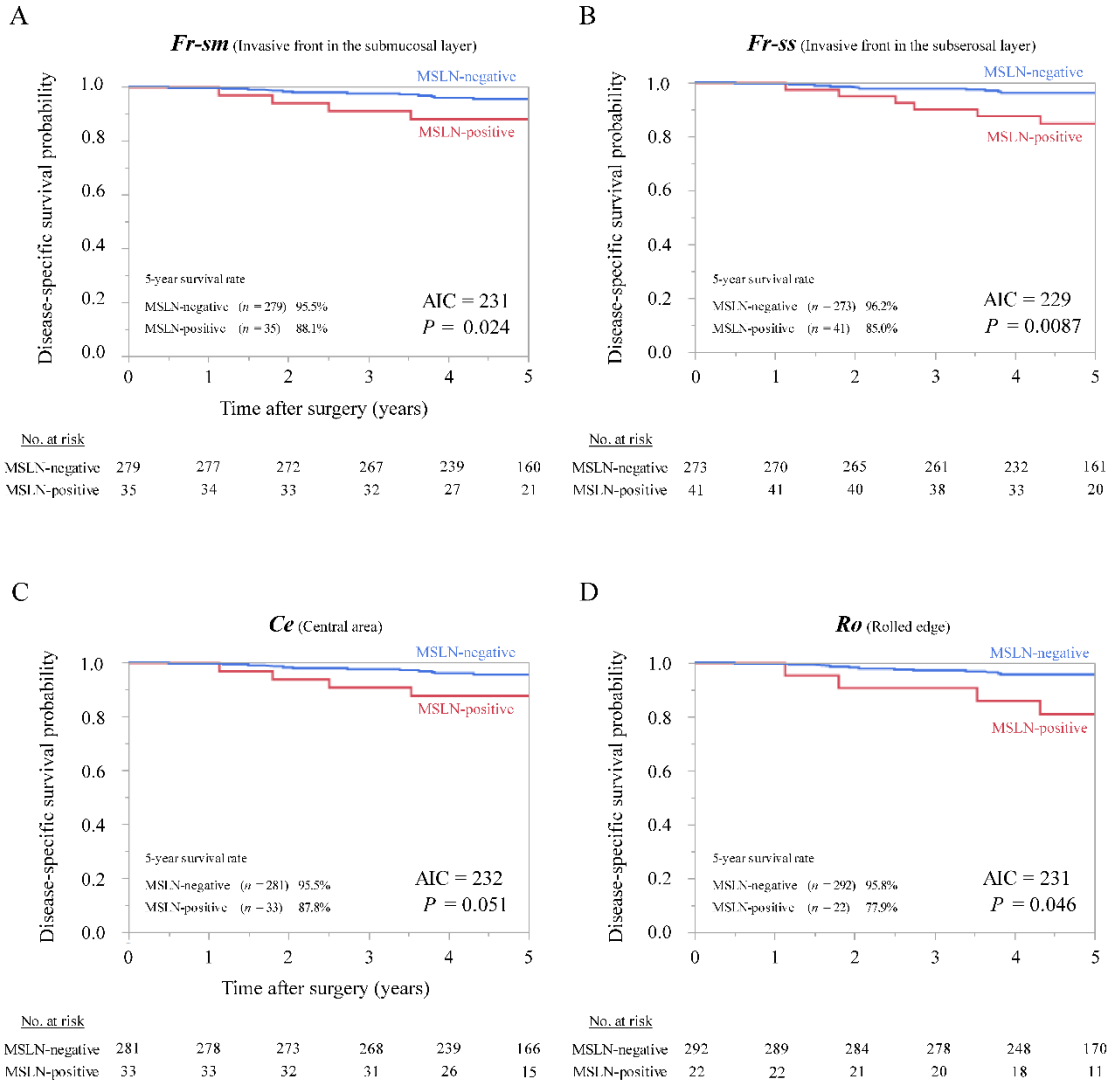

559

560

561

Table 1. Patients distribution and univariate analysis based on Cox's Proportional Hazards Model for disease-specific survival in Stage II colorectal cancer patients.

Variables	No. of cases	Univariate Analysis		
		Hazard Ratio	95% Confidence Interval	*P* value
Sex				
Male / Female	183 / 131	0.86	0.37 - 2.05	0.74
Age				
< 65 / ≥ 65	133 / 181	0.75	0.30 - 1.74	0.50
Location				
Right side / Left side	106 / 208	0.54	0.18 - 1.37	0.20
Histological grading [*1]				
G1, 2 / G3, 4	296 / 18	1.08	0.22 - 19.34	0.94
Depth of tumor [*1]				
T3 / T4	255 / 59	0.31	0.13 - 0.75	0.011
Venous invasion				
Negative / Positive	53 / 261	1.18	0.34 - 3.16	0.77
Lymphatic invasion				
Negative / Positive	27 / 287		Not Available [*4]	
Tumor budding [*2]				
Grade 1,2 / Grade 3	242 / 72	0.33	0.14 - 0.78	0.012
Microsatellite instability [*3]				
Low / High	300 / 14		Not Available [*4]	
Adjuvant chemotherapy				
Surgery alone / Chemotherapy	285 / 29	0.83	0.24 - 5.26	0.81

*1 TNM Classification (8th Edition, 2017)

*2 Japanese Classification of Colorectal Carcinoma (8th Edition, 2013)

*3 Microsatellite instability status was verified using immunohistochemical staining of MLH1 and MSH2

*4 All cases showing cancer-specific death were categorized as lymphatic invasion positive group and microsatellite instability low group

TABLE 2. Univariate and multivariate analyses based on Cox's Proportional Hazards Model for cancer-specific survival according to the clinicopathological features in different areas of Stage II colorectal cancers

Variables	No. of cases	Hazard Ratio	95% Confidence Interval	*P* value
Univariate Analysis				
Depth of tumor				
T3 / T4	255 / 59	0.31	0.13 - 0.75	0.011
Tumor budding				
Grade 1,2 / Grade 3	242 / 72	0.33	0.14 - 0.78	0.012
Mesothelin expression in ***Fr-sm***				
Negative / Positive	279 / 35	0.35	0.15 - 0.99	0.048
Mesothelin expression in ***Fr-ss***				
Negative / Positive	273 / 41	0.32	0.13 - 0.84	0.022
Mesothelin expression in ***Ce***				
Negative / Positive	292 / 22	0.38	0.15 - 1.17	0.087
Mesothelin expression in ***Ro***				
Negative / Positive	281 / 33	0.35	0.13 - 1.21	0.089
Multivariate Analysis				
Depth of tumor (T3 / T4)		0.38	0.14 - 0.82	0.035
Tumor budding (Grade 1,2 / Grade 3)		0.41	0.17 - 1.01	0.052
Mesothelin expression in ***Fr-sm*** (Negative / Positive)		0.53	0.21 - 1.52	0.22
Depth of tumor		0.36	0.16 - 0.90	0.027
Tumor budding		0.43	0.18 - 1.06	0.065
Mesothelin expression in ***Fr-ss***		0.46	0.19 - 1.23	0.12
Depth of tumor		0.36	0.16 - 0.89	0.027
Tumor budding		0.39	0.17 - 0.94	0.036
Mesothelin expression in ***Ce***		0.5	0.19 - 1.52	0.20
Depth of tumor		0.32	0.14 - 0.80	0.016
Tumor budding		0.35	0.15 - 0.85	0.021
Mesothelin expression in ***Ro***		0.28	0.10 - 0.99	0.049

569